Brain Pathology ISSN 1015–6305

RESEARCH ARTICLE

Association of adipocyte enhancer-binding protein 1 with Alzheimer's disease pathology in human hippocampi

Masahiro Shijo[1,2], Hiroyuki Honda[1], Satoshi O. Suzuki[1], Hideomi Hamasaki[1], Masaaki Hokama[3], Nona Abolhassani[4], Yusaku Nakabeppu[4], Toshiharu Ninomiya[5], Takanari Kitazono[2,5], Toru Iwaki[1]

[1] Department of Neuropathology, Neurological Institute, Graduate School of Medical Sciences, Kyushu University, Fukuoka, Japan.
[2] Department of Medicine and Clinical Science, Graduate School of Medical Sciences, Kyushu University, Fukuoka, Japan.
[3] Department of Neurosurgery, Japan Community Healthcare Organization, Kyushu Hospital, Fukuoka, Japan.
[4] Division of Neurofunctional Genomics, Department of Immunobiology and Neuroscience, Medical Institute of Bioregulation, Kyushu University, Fukuoka, Japan.
[5] Center for Cohort Studies, Graduate School of Medical Sciences, Kyushu University, Fukuoka, Japan.

Keywords
AE-binding protein 1, Alzheimer's disease, hippocampus, neurofibrillary tangle, neuron.

Corresponding author:
Toru Iwaki, MD, PhD, Department of Neuropathology, Neurological Institute, Graduate School of Medical Sciences, Kyushu University, 3-1-1 Maidashi, Higashi-ku, Fukuoka 812-8582, Japan (E-mail: *iwaki@np.med.kyushu-u.ac.jp*)

Received 11 May 2016
Accepted 5 December 2016
Published Online Article Accepted 20 December 2016

doi:10.1111/bpa.12475

Abstract

Adipocyte enhancer binding protein 1 (AEBP1) activates inflammatory responses via the NF-κB pathway in macrophages and regulates adipogenesis in preadipocytes. Up-regulation of AEBP1 in the hippocampi of patients with Alzheimer's disease (AD) has been revealed by microarray analyses of autopsied brains from the Japanese general population (the Hisayama study). In this study, we compared the expression patterns of AEBP1 in normal and AD brains, including in the hippocampus, using immunohistochemistry. The subjects were 24 AD cases and 52 non-AD cases. Brain specimens were immunostained with antibodies against AEBP1, tau protein, amyloid β protein, NF-κB, GFAP and Iba-1. In normal brains, AEBP1 immunoreactivity mainly localized to the perikarya of hippocampal pyramidal neurons, and its expression was elevated in the pyramidal neurons and some astrocytes in AD hippocampi. Although AEBP1 immunoreactivity was almost absent in neurons containing neurofibrillary tangles, AEBP1 was highly expressed in neurons with pretangles and in the tau-immunopositive, dystrophic neurites of senile plaques. Nuclear localization of NF-κB was also observed in certain AEBP1-positive neurons in AD cases. Comparison of AD and non-AD cases suggested a positive correlation between the expression level of AEBP1 and the degree of amyloid β pathology. These findings imply that AEBP1 protein has a role in the progression of AD pathology.

INTRODUCTION

Alzheimer's disease (AD) is a neurodegenerative disorder that accounts for the largest numbers of dementia cases. Since 1961, we have been conducting a long-term prospective cohort study of cerebro-cardiovascular diseases in the town of Hisayama, a suburb of Fukuoka in Japan. Previously, the Hisayama study has shown trends in the prevalence of AD and vascular dementia, and that both insulin resistance and dyslipidemia may be independent risk factors for plaque-type pathology (18, 19). We have expanded our observations of the molecular pathological alterations in AD brains by microarray analyses of post-mortem human brains donated to the Hisayama study (9). Extensive expression profiling using microarray analyses in a previous study revealed that adipocyte enhancer binding protein 1 (AEBP1) mRNA was significantly increased 2.68-fold in the AD hippocampus (9).

AEBP1 was originally identified in a mouse smooth muscle cell line as a transcriptional repressor with carboxypeptidase activity (7). Human AEBP1 was first identified as a gene whose cDNA is found exclusively in osteoblast and adipose tissue libraries (21). The predicted human AEBP1 protein had a nuclear targeting signal domain not seen in mouse Aebp1. Later it was revealed that AEBP1 was highly homologous to the C-terminus of aortic carboxypeptidase like protein (ACLP), a 1158-amino acid protein identified from aortic smooth muscle cells (13). Further observation revealed that AEBP1 and ACLP originate from the same gene, *AEBP1*, located on 7p13, suggesting that AEBP1 and ACLP (i.e., full-length AEBP1) expression is modulated mainly by alternative splicing (13, 23). In addition, full-length AEBP1 is predominantly secreted from smooth muscle cells to the extracellular matrix of mesenchymal cells (4, 5, 14), while the short isoform of AEBP1 appears to reside in the cytoplasm or nuclei and regulate intracellular signaling (13, 17). Diverse physiological functions of AEBP1 have previously been reported including the activation of inflammatory processes in macrophages by activating nuclear factor kappa B (NF-κB) (17), inhibition of peroxisome proliferator-

Table 1. Clinicopathological characteristics of the study subjects.

	AD ($n = 24$)	non-AD ($n = 52$)	*P*-value
Age at death (years)	89.0 ± 10.2	82.6 ± 6.1	0.0006
Male (%)	11 (45.83)	25 (48.08)	0.8555
Brain weight (g)	1128 ± 159.3	1209 ± 119.7	0.017
Post-mortem interval (h)	14.7 ± 10.9	16.1 ± 11.9	0.6155
CERAD senile plaque assessment			
None	0	16	
Sparse	0	20	
Moderate	0	5	
Frequent	24	11	
Braak and Braak staging			
1, 2	0	11	
3, 4	1	20	
5, 6	23	21	
Other dementia			
Vascular dementia	3	7	
Lewy body disease	2	2	
Other tauopathy *	1	14	
(no dementia)	0	35	

AD = Alzheimer's disease; CERAD = The consortium to establish a registry for Alzheimer's disease; * "Other tauopathy" includes argyrophilic grain disease and senile dementia with neurofibrillary tangles. Values are shown as mean ± standard deviation. Statistical comparisons between groups are performed using Welch's *t*-test (age at death, brain weight and post-mortem interval) or chi-square test (ratio of males).

activated receptor-gamma (PPAR-γ) and liver X receptor alpha (LXRα) (1, 16), regulation of adipogenesis via phosphatase and tensin homolog deleted from chromosome 10 (PTEN) in preadipocytes (11, 24, 33), abdominal wall development (3, 14) and lung fibrosis (26, 28). In mice, the short isoform of Aebp1 rather than the full-length isoform seems to have the activity of inflammatory processes in macrophages (1, 16, 17). However, the function of AEBP1 including the full-length isoform and the short isoform in physiological and pathological conditions in the human brain largely remains unknown.

In this study, we examined changes in the expression of AEBP1 in AD hippocampi using immunohistochemistry and immunoblotting to provide insight into the role of AEBP1 in the pathology of AD.

MATERIALS AND METHODS

Subjects

We examined 68 autopsy cases from Hisayama residents obtained from January 2013 to June 2014, and eight cases randomly selected from cases autopsied between 2009 and 2011. The total of 76 cases included 24 AD cases and 52 non-AD cases. The specimens included the middle frontal, superior and middle temporal gyri, inferior parietal lobule, hippocampus with entorhinal cortex and transentorhinal cortex at the coronal level of the lateral geniculate body, and the striate area. The *AEBP1* mRNA expression analysis was performed using seven AD and 10 non-AD autopsy samples from our previous study (9). The study was approved by the Ethics Committee of the Faculty of Medicine, Kyushu University.

Neuropathological assessment

The neuropathological examinations were performed as previously described (18). Briefly, formalin-fixed brain samples were embedded in paraffin and cut into 6 μm sections and stained with hematoxylin and eosin. AD pathology was assessed according to the Consortium to Establish a Registry for Alzheimer's disease (CERAD) guidelines (20) and the Braak and Braak neurofibrillary tangle (NFT) staging system (2). Clinicopathological characteristics of the study subjects are shown in Table 1.

Immunohistochemistry was performed using the following primary antibodies; anti-phosphorylated tau protein (clone AT8, mouse, monoclonal, 1:500, Innogenetics, Gent, Belgium), anti-amyloid β protein (clone 6F/3D; mouse, monoclonal, 1:100; Dako Cytomation, Carpinteria, CA, USA) and anti-AEBP1 (recognizing C-terminus side, 912-1014 amino acids of AEBP1, monoclonal, mouse, 1:333; ab54820; Abcam, Cambridge, UK). To unmask the epitope, sections were either autoclaved at 121°C for 10 minutes in 0.01 mol/L citrate buffer, pH 6 (for anti-AEBP1 and phosphorylated tau antibody) or dipped in 90% formic acid for 60 minutes (for anti-amyloid β protein antibody). Specimens were incubated with the primary antibodies at 4°C overnight, and the signal visualized using an enhanced indirect immunoperoxidase method (EnVision + System; Dako). Nuclei were counterstained with hematoxylin.

Double immunofluorescence was performed using combinations of primary antibodies against AEBP1/4-repeat tau (CAC-TIP-4RT-P01; rabbit, polyclonal, 1:1500; Cosmo Bio, Tokyo, Japan), AEBP1/glial fibrillary acidic protein (GFAP) (Z0334; rabbit, polyclonal, 1:250; Dako), AEBP1/S-100 protein (NCL-L-S100p, rabbit, polyclonal, 1:200; Leica Biosystems, Newcastle, UK), AEBP1/ionized calcium-binding adaptor molecule 1 (Iba-1) (019-19741; rabbit, polyclonal, 1:250; Wako, Osaka, Japan), AEBP1/CD45 (LCA) (M0701, mouse, monoclonal, 1:50; Dako) and AEBP1/NF-κB p50 component (ab32360; rabbit, monoclonal, 1:100; Abcam). The signal was visualized using appropriate secondary antibodies conjugated to Alexa Fluor dyes (1:50; Thermo Fisher Scientific, Waltham, MA, USA), or the Opal™ 3-plex kit using fluorescein, cyanine 3 and cyanine 5 (NEL791001KT, PerkinElmer, Waltham, MA, USA). Nuclei were counterstained with 4′,6-diamidino-2-phenylindole (DAPI). The specimens were examined using a confocal laser microscope (A1 Confocal Laser Microscope, Nikon Corporation, Tokyo, Japan).

Image analyses of immunoreactivity for AEBP1

We semiquantitatively evaluated AEBP1 immunoreactivity in the brains of three AD and three non-AD cases. AEBP1-immunoreactivity was defined as follows: (−), no AEBP1-immunopositive structures; (+), over half the cells weakly immunopositive for AEBP1; (++), many cells immunopositive for AEBP1 with variable staining intensities; (+++), almost all cells strongly immunopositive for AEBP1 (examples are shown in Supporting Information Figure S1). We could not examine spinal cords because these samples were not included in the autopsy cases of the Hisayama study. Instead, we performed immunohistochemistry for AEBP1 on a spinal cord obtained from a non-demented patient (a 46-year-old man with Becker muscular dystrophy).

Immunoreactivity for AEBP1 in human hippocampi was quantitatively evaluated. Photomicrographs of each specimen were taken in the CA1–4 subfields, subiculum and entorhinal cortex at 200×, magnification using a digital microscope camera (DP21; Olympus, Tokyo, Japan) mounted on a light microscope (BX41; Olympus). Images were analyzed using ImageJ ver 1.48 (http:/rsb.info.nih.gov/ij) as follows. The size of each image was 1600 × 1200 pixels and the photographed area was 3.632 × 2.724 mm^2. The hematoxylin staining was separated from the DAB coloring using the Color Deconvolution plugin (25). For each image, we manually set the highest threshold for the selection of regions of interest at which the background staining was sufficiently eliminated. We then measured the mean gray value and ratio of the stained area to the total area. The optical density (OD) of each image was defined as the difference between the mean gray value of the total microscopic field and the highest gray value of the ROI. We employed the OD in area CA4 (OD_{CA4}) as the internal control because the staining intensity was strong and constant in this area across the specimens. We compared the relative ODs (% of OD_{CA4}) of each region between the cases.

Western blotting

Hippocampal tissues from four AD cases and four non-AD cases from the current case series were sampled at autopsy. For control samples, we separately obtained aorta, adrenal gland, cerebral cortex of frontal lobe and hippocampal tissues from a non-demented patient (a 46-year-old man with Becker muscular dystrophy) from the Department of Neurology, Neuro-Muscular center, National Omuta Hospital. The samples were snap frozen and stored at −80°C until use. The brain samples were homogenized at 5000 rpm for 30 s in a bead disrupter homogenizing system (Micro Smash MS-100; Tomy Seiko Co., Ltd, Tokyo, Japan) to a final concentration of 10% in lysis buffer (50 mM Tris-HCl pH 6.8, 2 mM EDTA, 2 mM PMSF, 0.5% Triton-X, PhosSTOP [Roche, Indianapolis, IN, USA] and cOmplete™ (Roche)). The homogenates were then clarified by centrifugation at 2100 × g for 5 minutes and the supernatant was stored at −80°C. For the aorta and adrenal gland tissues, we performed an additional acetone precipitation to remove excess lipid. The lysate was mixed in four volumes of acetone, incubated at −80°C for 60 minutes and centrifuged at 10 000 × g for 15 minutes. The supernatant was aspirated and the precipitate was dried and dissolved in lysis buffer. In addition, we used hippocampal lysates from four AD cases and four non-AD cases diluted in radioimmunoprecipitation assay buffer (150 mM NaCl, 50 mM Tris-HCl pH 8.0, 1.0% Nonidet™ P-40, 0.5% sodium deoxycholate and 0.1% SDS) as described in our previous experiment (9).

The lysate was mixed with 50% LDS sample buffer (Thermo Fisher Scientific) containing 5% 2-mercaptoethanol, and heated to 95°C for 5 minutes. The lysate was separated in a 10% tris-glycine extended gel (Bio-Rad, Hercules, CA, USA) and transferred onto polyvinylidene difluoride membrane (Bio-Rad). The membranes were incubated with 5% skim milk diluted in tris-buffered saline, 0.1% Tween 20 for 60 minutes at room temperature and probed with the following primary antibodies for 1 h at room temperature: AEBP1 C-terminus, amino acids 912–1014 (ab54820; mouse, monoclonal, 1:1500; Abcam); AEBP1 N-terminus, amino acids 341–372 (LS-C156122; rabbit, polyclonal, 1:1000; Lifespan BioScience, Seattle, WA, USA) and cyclophilin B (ab178397; rabbit, monoclonal, 1:5000; Abcam). After rinsing, the membranes were incubated with peroxidase-conjugated secondary antibodies (AP192P; anti-mouse IgG, 1:10 000; Merck Millipore, Darmstadt, Germany; or #170-6515; anti-rabbit IgG, 1:10 000; Bio-Rad) for 1 h at room temperature. Immunoreactivity was visualized using Enhanced Chemiluminescence Plus Western Blotting Detection Reagent (GE Healthcare; Chalfont St. Giles, UK) according to the manufacturer's instructions. The relative amount of AEBP1 protein to the loading control cyclophilin B, was measured by densitometry using the Light Capture System II, CS Analyzer (ver 2) (Atto, Tokyo, Japan).

mRNA expression analysis

Total RNA was isolated and the expression profile of *AEBP1* mRNA was determined as described previously (9). According to the Emsembl database (http://www.ensembl.org) (32) based on the human genome assembly GRCh38, *AEBP1* gene has four protein-coding transcripts including mRNA1 (4081 base pairs (bp), consisting of 21 exons, coding the full-length 1158-amino acid protein), mRNA2 (2571 bp, consisting of exons 12–21 and retained introns 12 and 13 of mRNA1, coding a 733-amino acid protein), mRNA3 (751 bp, consisting of exons 1–3 and 6–8 of mRNA1, coding a 251-amino acid protein) and mRNA4 (566 bp, consisting of exons 2–4 and retained intron 1 of mRNA1, coding a 162-amino acid protein). Of the proteins translated from these protein-coding mRNA, only the products derived from mRNA1 and mRNA2 could be examined using immunohistochemistry (ab54820, recognizing the C-terminus 912–1014 amino acids of AEBP1). Therefore, we focused our investigation on mRNA1 and mRNA2. The first exon of mRNA2 consists of exons 12, 13 and 14 and retained introns 12 and 13 of mRNA1. To examine which splice variants of *AEBP1* were expressed in human hippocampi, we performed reverse-transcription polymerase chain reaction (RT-PCR) using primers crossing exons 12 and 13 (forward, 5′-ACAGCCAGACATGGGTGATG-3′; reverse, 5′-GTCCTTGTC CACGTTCCCAT-3′; product lengths: mRNA1, 71 bp, mRNA2, 174 bp) and exons 13 and 14 of mRNA1 (forward, 5′-GCATCTACCCACTCACCTGG-3′; reverse, 5′-ACCTCATTC TGTGCGTAGTAGC-3′; product lengths: mRNA1, 100 bp, mRNA2, 196 bp). Each sample was reverse-transcribed to first strand cDNA using 1 μg of total RNA, random primers and the High-Capacity cDNA Reverse-Transcription Kit (Life Technologies Japan, Tokyo, Japan). Each PCR reaction was performed using 0.5% of the total complementary DNA, forward and reverse primers (primer set #1, 200 nM; primer set #2, 50 nM) and 10 μL of THUNDERBIRD SYBR qPCR Mix (Toyobo, Tokyo, Japan) in a total volume of 20 μL, using a Thermal Cycler Dice Real-Time System Single (Takara, Kyoto, Japan). The PCR reaction was performed as follows: a single cycle of 95°C for 30 s, and 40 cycles of 95°C for 5 s and 60°C for 1 minute. Specificity of the PCR products was established by dissociation curve analysis, and sizes verified on a 2.5% agarose gel.

Statistical analysis

All values are expressed as means ± standard deviations (SD) or medians [95% confidence intervals]. Statistical comparisons between groups were performed using Welch's *t*-tests or Wilcoxon rank sum tests for the single-group comparison of the numerical values, one-way analysis of variance (ANOVA) followed by

Tukey–Kramer honest significant difference (HSD) test for the multi-group comparison of the numerical values, or chi-square test for the single-group comparison of the categorical values using JMP software (Version 11, SAS Institute, Cary, NC, USA). Probability values of <0.05 were considered statistically significant.

RESULTS

AEBP1 expression in the human central nervous system

The immunohistochemical profiles of AEBP1 in the human central nervous system were investigated in three AD, three non-AD cases and a control cases (Table 2), and representative photomicrographs are shown in Figure 1. We observed expression of AEBP1 in the perikarya of pyramidal neurons in the hippocampal formation, cerebral cortex, basal ganglia, thalamus and brainstem. AEBP1-immunopositive astrocytes and microglia were also seen in some cases although both the immunoreactivity intensity and frequency of AEBP1-immunopositive cells were lower than those in pyramidal neurons. In contrast, Purkinje and granular cells in the cerebellar cortex were almost immunonegative, whereas Bergmann glia were moderately immunopositive. Choroid plexus epithelial cells were also immunopositive for AEBP1 as previously described (14). The difference in AEBP1immunoreactivity between AD and non-AD cases seemed to be most evident in the hippocampal formation. In the spinal cord, pyramidal neurons of the ventral and dorsal horns were immunopositive for AEBP1, with no evident AEBP1-immunopositive structures in the white matter.

AEBP1 expression in human hippocampi

We observed expression of AEBP1 in the perikarya of pyramidal neurons in the hippocampi, subiculum and entorhinal cortex as well as in granule cells of the dentate gyrus in both the AD and non-AD groups (Figure 2). In the non-AD group, the immunoreactivity for AEBP1 was weaker in area CA1, the subiculum and the entorhinal cortex compared with areas CA4, CA3 and CA2 (Figure 2A–G). AEBP1-postive glial cells were also sparsely distributed throughout these regions. In the AD group, expression of AEBP1 in pyramidal neurons was elevated in all regions, and AEBP1-postive glial cells were also increased (Figure 2H–N). These AEBP1-immunopositive structures were not detected in negative controls without the primary antibody (see Supporting Information Figure S2).

The relationship between AD pathology and AEBP1 expression

Neurofibrillary tangles (NFTs) were immunonegative for AEBP1, and AEBP1 immunoreactivity was weakened in the perikarya of NFT-bearing neurons (Figure 3A, arrowhead). Double immunofluorescence for AEBP1 and 4-repeat tau in area CA1 also showed that AEBP1 was depleted in neurons bearing NFTs (Figure 3B–D, arrowheads). However, neurons with pretangles, revealed by diffuse staining for tau protein in neuronal somata, appeared to have elevated expression of AEBP1 (Figure 3B–D, arrows).

In senile plaques, club-like, AEBP1-immunopostive structures were observed, while amyloid cores were immunonegative for AEBP1 (Figure 3A, arrow). AEBP1 and amyloid β protein immunohistochemistry in serial sections confirmed the localization of AEBP1-immunoreactivity to neuritic plaques, whereas the distribution of AEBP1 was different to that of amyloid β protein (Figure 3E,F). These AEBP1-immunopositive structures in senile plaques were observed more frequently in area CA1, the subiculum and the entorhinal cortex than in the other subfields of the hippocampus and the parahippocampal cortices. Double immunofluorescence for AEBP1 and 4-repeat tau showed partial co-localization of the proteins. AEBP1 was expressed mainly in neurites with diffuse staining for 4-repeat tau protein, but depleted in neurites containing solid tangles. (Figure 3G–I). These AEBP1-immunopositive structures in senile plaques were not detected in negative controls without the primary antibody (see Supporting Information Figure S2).

An overlap of AEBP1-, GFAP- and S-100 protein-immunopositivity was noted in the cytoplasm of astrocytes. We also observed co-localization of small AEBP1-immunopositive structures in some Iba-1- and LCA-positive microglial cell bodies. However, the AEBP1 immunoreactivity in senile plaques did not colocalize with astrocyte markers and microglia markers (see Supporting Information Figure S3).

We also found that certain AEBP1-immunopositive neurons in the AD group showed nuclear localization of NF-κB. Conversely, in glial cells no definite nuclear localization of NF-κB was observed regardless of AEBP1 expression. In contrast, nuclear localization of NF-κB in neurons of non-AD group was not evident (Figure 4).

Quantitative comparison of AEBP1 immunoreactivity in AD and non-AD groups

We quantitatively compared AEBP1 immunoreactivity in the hippocampi of AD and non-AD groups (Figure 5A–C). The mean OD in area CA4 was similar in the AD and non-AD groups (AD group, 25.57 ± 7.05; non-AD group, 25.86 ± 7.46; $P = 0.876$; Figure 5D). The difference in the mean area of AEBP1-immunopositive structures in area CA4 was not significant between the groups (% of photographed area; AD group, 3.39 ± 1.08; non-AD group, 3.38 ± 1.05; $P = 0.984$, Figure 5D). We, thus, defined the OD in the CA4 area (OD_{CA4}) as the internal control for each specimen, and compared the relative ODs of each region as a percentage of the OD_{CA4} in both the AD and non-AD groups.

AEBP1 immunoreactivity in different AD and non-AD brain regions is shown in Figure 5E–I. The OD of AEBP1 (% of OD_{CA4}) in AD cases was significantly higher than in non-AD subjects in areas CA3 (AD, 102.71 ± 13.72; non-AD, 95.46 ± 12.09; $P = 0.0321$) and CA1 (AD, 80.90 ± 18.92; non-AD, 69.29 ± 10.80; $P = 0.0088$), the subiculum (AD, 76.91 ± 15.69; non-AD, 59.73 ± 10.00; $P < 0.0001$) and entorhinal cortex (AD; 86.62 ± 24.57; non-AD, 72.85 ± 12.8; $P = 0.0149$), but not in area CA2 (AD, 104.34 ± 14.03; non-AD, 102.52 ± 14.97; $P = 0.614$). The area of AEBP1-immunopositivity (% of photographed area) in AD cases was also significantly larger in area CA1 (AD, 3.23 ± 1.02; non-AD, 2.36 ± 1.22; $P = 0.0021$), the subiculum (AD, 3.68 ± 1.49; non-AD, 1.76 ± 0.93); $P < 0.0001$) and the entorhinal cortex (AD, 4.13 ± 1.89; non-AD, 2.40 ± 1.25; $P = 0.0003$).

To analyze the changes in AEBP1-expression due the pathological progression of AD, we compared relative OD and AEBP1-positive areas in different CERAD senile plaque assessment stages (N, S, none and sparse, $n = 36$ vs. M, F, moderate and frequent; $n = 40$) and Braak and Braak NFT stages (stages 1 and 2, $n = 11$;

Table 2. Immunohistochemical profiles of AEBP1 in human brains.

	AD			nAD		
	Case 1	Case 2	Case 3	Case 1	Case 2	Case 3
age at death (years)	101	100	89	59	87	84
sex	M	F	F	F	M	F
Post-mortem index (minute)	1012	308	1470	650	1233	756
CERAD plaque assessment	Frequent	Frequent	Frequent	None	None	None
Braak and Braak NFT stage	6	5	5	1	4	4
hippocampal formation						
dentate gyrus	+	+	+	+	+	−
CA4	+++	+++	+++	+++	++	++
CA3	+++	+++	+++	++	++	++
CA2	+++	+++	+++	++	++	++
CA1	+++	+++	+++	+	+	+
subiculum	+++	+++	++	+	+	+
entorhinal cortex	++	++	++	+	+	+
transentorhinal cortex	+	++	+	+	+	+
cerebral cortex						
neuron	++	+++	+++	+	++	++
astrocyte	+	+	++	+	+	+
oligodendrocyte	−	−	−	−	−	−
microglia	+	+	+	−	+	−
endothelium	−	−	−	−	−	−
smooth muscle cell	−	−	−	−	−	−
arachnoid cell	−	+	−	−	+	−
cerebral white matter						
astrocyte	++	++	++	+	+	+
oligodendrocyte	−	−	−	−	−	−
endothelium	−	−	−	−	−	−
smooth muscle cell	−	−	−	−	−	−
ependymal cell	−	−	+	+	−	−
choroid plexus epithelial cell	+++	+++	+++	+++	+++	+++
cerebellum						
Purkinje cell	−	+	−	+	+	−
Bergmann glia	+	++	++	++	++	++
granular cell	−	−	−	+	−	+
dentate nucleus	+	+	+	+	+	+
Neurons in other regions						
putamen	++	++	+	+	++	+
globus pallidus	++	++	+++	+	+	++
Meynert's nucleus	+++	+++	+++	++	+++	+++
amygdala	++	+++	+++	+	+++	+++
thalamic nuclei	+++	++	++	++	++	++
subthalamic nucleus	+++	+++	++	++	+	+++
substantia nigra	+	++	++	−	+	+
oculomotor nucleus	++	+++	+++	+++	+++	++
locus coeruleus	−	+	−	−	−	−
raphe nuclei	+	+	++	++	++	++
pontine nuclei	+	+	+	++	+	++
hypoglossal nucleus	++	+++	++	++	+++	+++
dorsal vagal nucleus	++	+++	++	+	+	+
inferior olivary nucleus	+++	+++	+++	++	+++	+++

AD = Alzheimer's disease; CERAD = The Consortium to Establish a Registry for Alzheimer's Disease; NFT = neurofibrillary tangle.

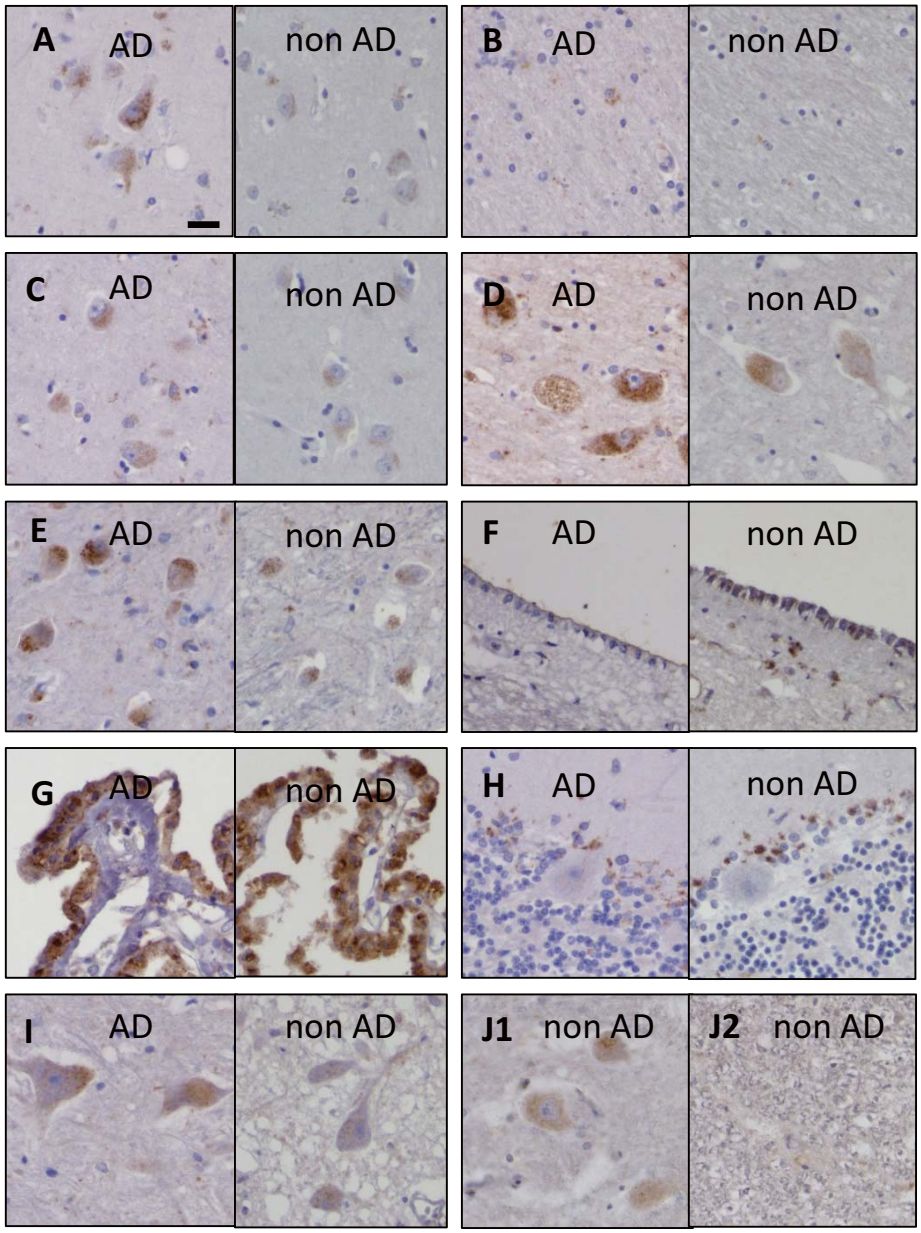

Figure 1. Distribution of AEBP1 protein expression in the human central nervous system. **(A–I)** Immunohistochemistry for AEBP1 in an AD subject (AD case 1 in Table 2) and a non-AD subject (non-AD case 1 in Table 2). **(A)** cerebral neocortex, **(B)** cerebral white matter, **(C)** amygdala, **(D)** basal nucleus of Meynert, **(E)** thalamic nuclei, **(F)** ependymal cells, **(G)** choroid plexus, **(H)** cerebellar cortex, **(I)** dorsal vagal nucleus. **(J1** and **2)** Immunohistochemistry for AEBP1 in the eighth cervical spinal cord of a non-demented patient (46-year-old man with Becker muscular dystrophy). **(J1)** pyramidal neurons of the ventral horn, **(J2)** the lateral funiculus. Bars = 20 μm.

stages 3 and 4, $n = 21$; stages 5 and 6, $n = 44$). The AEBP1 OD (% of OD_{CA4}) and AEBP1-positive area (% of photographed area) in area CA1 were not significantly different over the senile plaque stages (OD: N, S, 70.71 ± 11.46; M, F, 74.98 ± 17.13; $P = 0.211$, area: N, S, 2.34 ± 1.41; M, F, 2.90 ± 0.974; $P = 0.0517$; Figure 6A) or NFT stages (OD: stages 1 and 2, 71.32 ± 10.71; stages 3 and 4, 71.29 ± 12.64; stages 5 and 6, 74.16 ± 16.63; $P = 0.712$, area: stages 1 and 2, 2.14 ± 1.24; stages 3 and 4, 2.62 ± 1.37; stages 5 and 6, 2.77 ± 1.14; $P = 0.314$; Figure 6B), although the AEBP1-positive area tended to be larger in the later CERAD stages. In the subiculum, the OD of AEBP1 and AEBP1-positive area increased along with the progression of senile plaque pathology (OD: N, S, 60.68 ± 9.99; M, F, 69.18 ± 16.61; $P = 0.0094$; area: N, S, 1.70 ± 0.97; M, F, 2.96 ± 1.54; $P < 0.001$; Figure 6C). The AEBP1-positive area in the subiculum also increased significantly along with the progression of NFT pathology (stages 1 and 2, 1.30 ± 0.70; stages 3 and 4, 1.97 ± 0.91; stages 5 and 6, 2.82 ± 1.59; $P = 0.0017$; Figure 6D). The OD in the subiculum tended to be higher in cases in Braak stages 5 or 6 than in those in other stages; however, there was no significant difference (stages 1

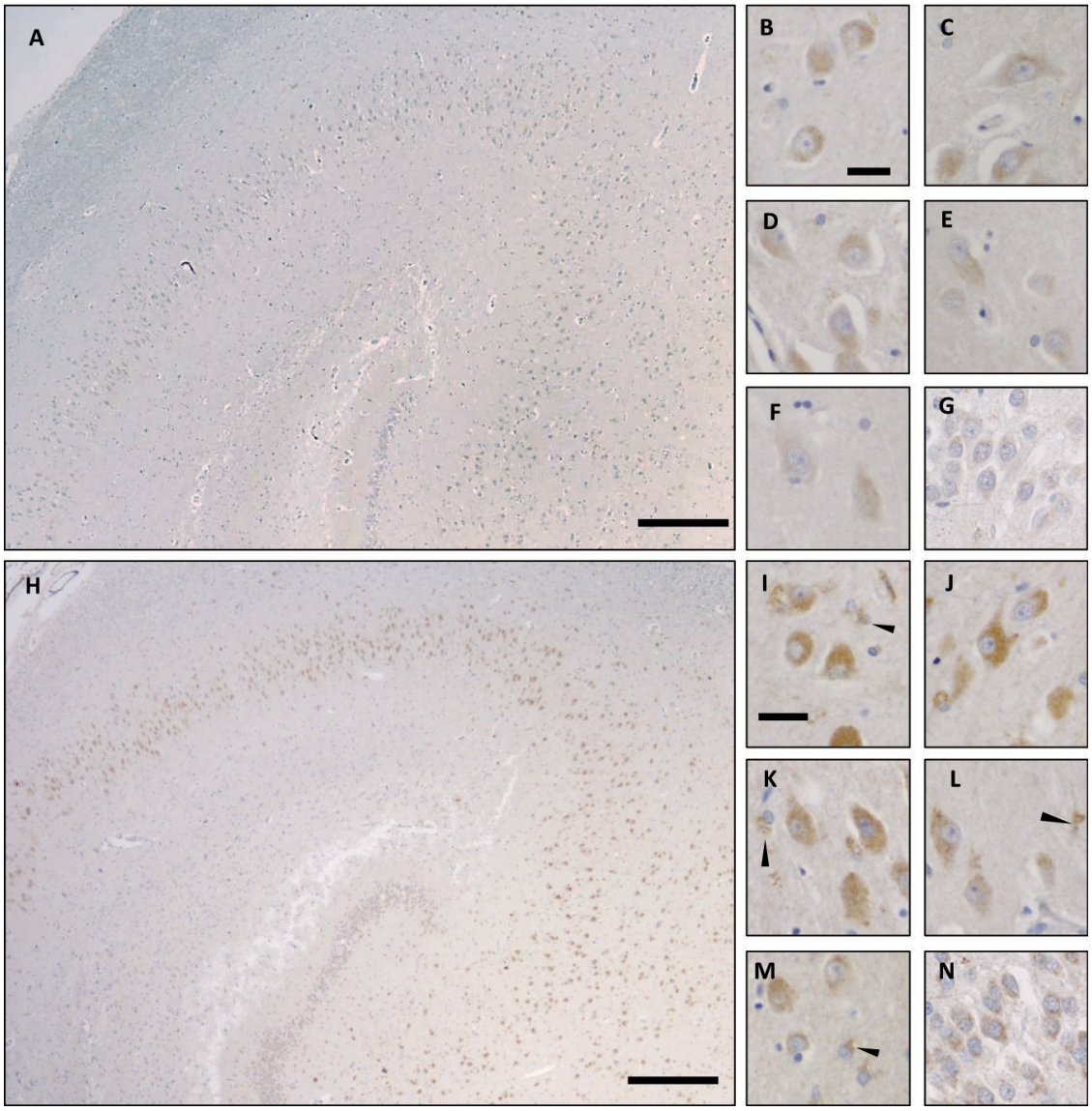

Figure 2. Immunohistochemistry for AE-binding protein (AEBP1) in human hippocampi and parahippocampal cortices of a non-AD subject (**A–G**) and an AD case (**H–N**). **(A, H)** Low-power images of CA2–CA4 subfields. **(B–G, I–N)** High-power images of the CA4 (**B, I**), CA3 (**C, J**), CA2 (**D, K**) and CA1 (**E, L**) regions, the subiculum (**F, M**) and dentate gyrus (**G, N**). AEBP1 is localized in neuronal perikarya. In a non-AD subject, immunoreactivity for AEBP1 was weak in area CA1 (**E**) and the subiculum (**F**) compared with areas CA2–CA4 (**B–D**). In one AD case, immunopositivity for AEBP1 was increased in neurons in each hippocampal subfield and in some glial cells (arrowheads in **I–N**). **(A, H)** bars = 300 μm. **(B–G, I–N)** bars = 20 μm.

and 2, 59.36 ± 7.39; stages 3 and 4, 61.45 ± 10.05; stages 5 and 6, 68.37 ± 16.67; $P = 0.0675$; Figure 6D). In the entorhinal cortex, the AEBP1-positive area significantly increased along with the progression of senile plaques although the OD was not significantly different (OD: N, S, 75.01 ± 13.10; M, F, 79.17 ± 22.07; $P = 0.317$; area: N, S, 2.37 ± 1.35; M, F, 3.46 ± 1.79; $P = 0.0034$; Figure 6E). The AEBP1-positive area in the entorhinal cortex also increased significantly along with the progression of NFT (area: stages 1 and 2, 1.46 ± 0.57; stages 3 and 4, 2.48 ± 0.97; stages 5 and 6, 3.54 ± 1.83; $P = 0.0002$; Figure 6F). The OD in the entorhinal cortex tended to be larger in cases in Braak stages 5 or 6 than in those in other stages. However, Tukey–Kramer HSD *post hoc* analysis failed to reveal a significant difference (stages 1 and 2, 69.48 ± 9.86; stages 3 and 4, 71.56 ± 11.76; stages 5 and 6, 81.82 ± 21.21; $P = 0.033$; Figure 6F).

AEBP1 immunoblotting

Immunoblotting with aortic lysate from the normal control case showed bands at both 130 kDa and 170 kDa, corresponding to the molecular weights of the full-length protein (4) and its glycosylated form (13), respectively. The band around 83 kDa, corresponding to the molecular weight of the short isoform (15), was also seen. In contrast, immunoblotting with lysates from the adrenal gland from

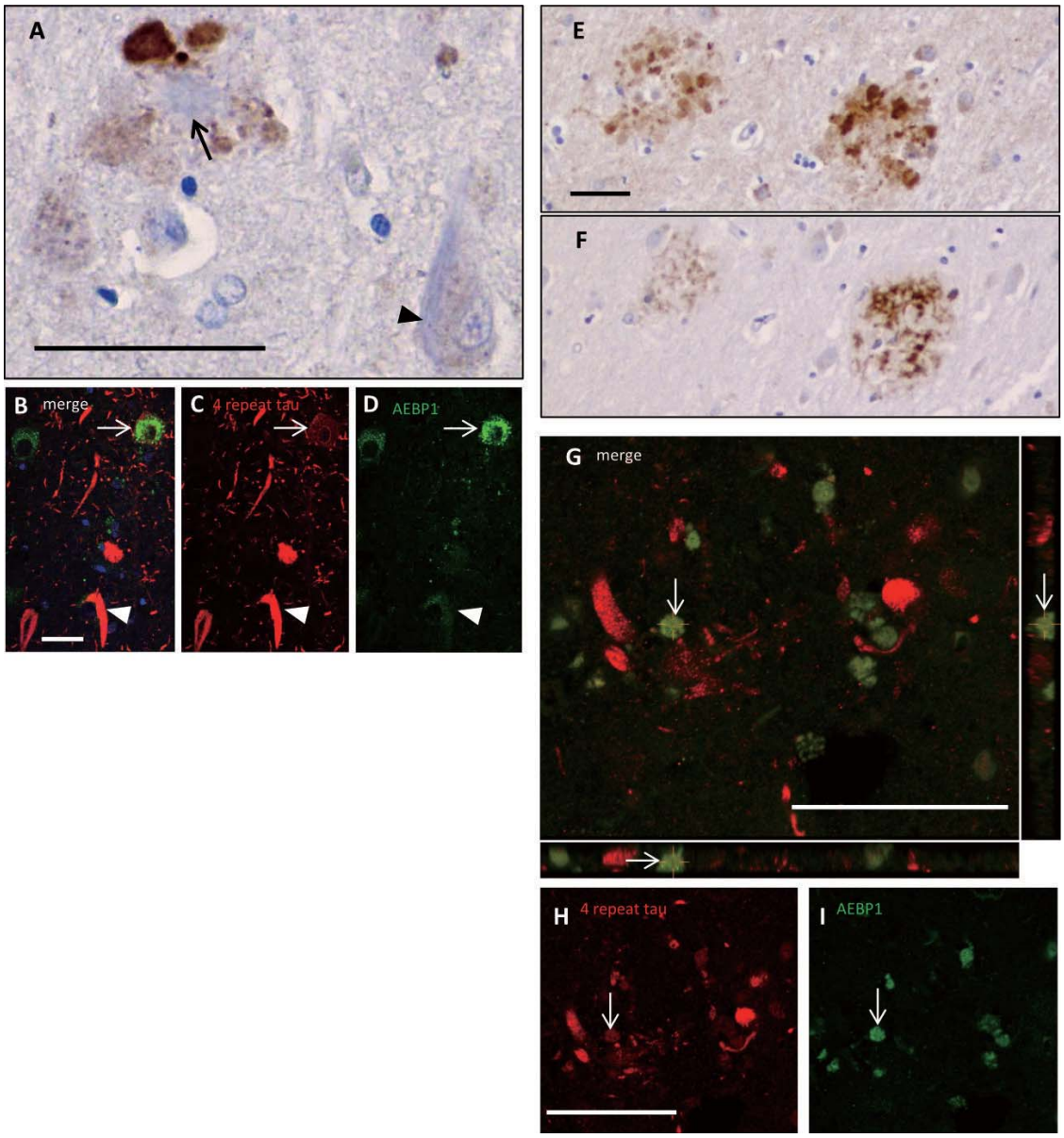

Figure 3. Distribution of the AEBP1 protein in neuritic plaques and in tangle-bearing neurons. **(A)** Immunohistochemistry for AEBP1 in the hippocampi of AD cases. **(B–D)** Double immunofluorescence for AEBP1 (green) and 4-repeat tau (red) in area CA1. **(E, F)** Immunohistochemistry for AEBP1 (**E**) and amyloid β protein (**F**) on serial sections. **(G–I)** Double immunofluorescence for AEBP1 (green) and 4-repeat tau (red) in a neuritic plaque. Neurofibrillary tangles (NFTs) are immunonegative for AEBP1 (arrowheads in **A–D**) and AEBP1 is markedly depleted in neurons bearing NFTs. In contrast, neurons with pretangles are positive for AEBP1 (arrows in **B–D**). Club-like, AEBP1-immunoreactive structures are observed around an AEBP1-immunonegative amyloid core (arrow in **A**). AEBP1 protein is deposited in neuritic plaques, however, the distribution is somewhat different to that of amyloid β protein (**E, F**). Double immunofluorescence shows a partial co-localization of AEBP1 and 4-repeat tau protein in a neuritic plaque (**G–I**). Cross sections of z-stacked images of the structure pointed by arrow are shown in the right and lower side of (**G**). Bars = 50 μm.

the same case only showed a band around 83 kDa. In the hippocampus and frontal cortex, AEBP1-immunoblotting revealed a band around 83 kDa and another with a lower signal intensity around 170 kDa. These signals were not detected when immunoblotting without the primary antibody (Supporting Information Figure S4A). AEBP1-immunoblotting with hippocampal lysates from another set of AD and non-AD subjects sampled during 2013–2014 also revealed bands around 83 kDa, as well as around 170 kDa, without significant differences between each group in the amount of the protein (data not shown). We performed additional immunoblotting with hippocampal lysates from the previous study, in which the expression levels of *AEBP*1 mRNA had been already analyzed (9). This immunoblotting with anti-AEBP1 antibody recognizing amino acids 912–1014 of the full-length protein (an

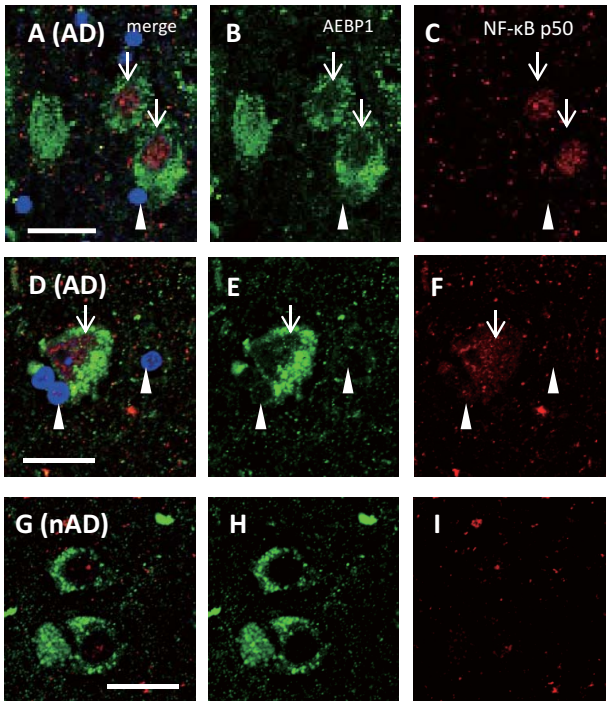

Figure 4. Double immunofluorescence for AEBP1 (green) and NF-κB p50 domain (red) in the subiculum in Alzheimer's disease (**A–F**) and in non-dementia case (**G–I**). In AD cases, nuclear localization of NF-κB is noted in some of AEBP1-immunopositive neurons (arrows). In glial cells, no definite nuclear localization of NF-κB is observed (arrowheads). In non-AD cases, nuclear accumulation of NF-κB in neurons is not observed (**G–I**). Bars = 20 μm.

epitope within a domain common to the full-length and short isoforms) showed bands around both 83 kDa and 170 kDa. Each of the proteins probed was also detected with another anti-AEBP1 antibody recognizing amino acids 341–372 of the full-length protein (an epitope within a full-length-specific domain) (Supporting Information Figure S4B). As the 83-kDa band was detected with both antibodies, it is possible that this band represents a truncated product of the full-length AEBP1, rather than a product from a short splice variant mRNA. Several extra bands were also seen in each experiment, probably derived from serum immunoglobulin, auto-proteolytic products during post-mortem periods, or unknown post-translational modification products.

mRNA expression profiles of AEBP1 in human hippocampi

The microarray analysis in the previous experiment (9) showed a greater expression of *AEBP1* mRNA in human AD hippocampi than in non-AD hippocampi (by-weight average signal ($\log_2$): AD, 9.75 [8.55–11.02]; non-AD, 8.69 [8.50–9.36], $P = 0.011$; Figure 7A). The quantitative RT-PCR (qRT-PCR) in our previous experiment (9) showed that the relative expression level of *AEBP1* mRNA appeared to increase in AD cases, but without statistical significance (ratio AD:non-AD, 1.99, $P = 0.330$). The primers in the previous qRT-PCR were designed to join exon 14 of mRNA1 and thus were able to amplify both mRNA1 and mRNA2, so it was unclear which transcript had altered expression levels during AD pathological changes. RT-PCR using primer set #1 (flanking the junction of exons 12–13 of mRNA1) and set #2 (flanking the junction of exons 13–14 of mRNA1) showed that both primer sets could amplify the fragments corresponding to *AEBP1* mRNA1. In contrast, fragments corresponding to mRNA2 were amplified only with primer set #1. We tried additional experiments using higher concentrations of primer set #2 (up to 200 nM); however, the fragments corresponding to mRNA2 were still not observed (data not shown). These findings suggest: (1) the *AEBP1* mRNA isolated from human hippocampi contained mRNA1, but the mRNA2 containing introns 12 and 13 is not expressed in human hippocampi (Figure 7B,C); (2) the qRT-PCR result in our previous experiment (9) reflected the expression level of *AEBP1* mRNA1, but not that of mRNA2; (3) the 83-kDa protein observed by immunoblotting seemed to be derived from the full-length protein through unknown processes such as post-translational modification and/or auto-proteolysis during the post-mortem period, rather than the short isoform of AEBP1 translated from mRNA2.

DISCUSSION

This study revealed that the expression of AEBP1 protein in the human central nervous system occurred mainly in neurons, and was elevated in neurons and some glial cells of hippocampi and parahippocampal cortices in association with AD pathological changes. RT-PCR revealed that in human brain, the major transcript of *AEBP1* gene was mRNA1 (coding full-length protein) rather than mRNA2 (coding short isoform protein) and the full-length AEBP1 protein existed in human brain. AEBP1 protein accumulates in senile plaques and neuronal somata, most frequently in those containing pretangles (indicated by diffuse perikaryal immunostaining for tau protein). AEBP1-immunoreactivity increased mainly, in area CA1, the subiculum and the entorhinal cortex of AD cases, as amyloid β- and tau-associated pathological changes progressed. This suggests the AEBP1 protein may play a role in the progression of AD pathology.

Regarding the constitutive expression of AEBP1 in brain tissue, previous reports have shown that AEBP1 protein is expressed in the choroid plexus of embryos (14) and in some glioma cell lines (12). However, the expression profile of the AEBP1 protein in adult brains has not yet been examined. This is the first report describing neuronal expression of AEBP1 protein in the adult human central nervous system. AEBP1-immunoreactivity appears to be higher in the neurons of areas CA2, CA3 and CA4 than in area CA1, the subiculum, or the entorhinal cortex. This heterogeneous expression pattern suggests differential functions of AEBP1 protein in each subfield of the hippocampus.

In AD brains, both neurons and glial cells in the affected hippocampi showed increased AEBP1-immunoreactivity compared to those in non-AD cases. This alteration of AEBP1 protein expression in the hippocampus of AD cases parallels AEBP1 mRNA expression (9). Notably, the increase of AEBP1-immunoreactivity mainly occurred in the area CA1, the subiculum and the entorhinal cortex. These regions are the primary sites of lesions in AD pathology, and the AEBP1 protein accumulated in senile plaques and neurons with pretangles.

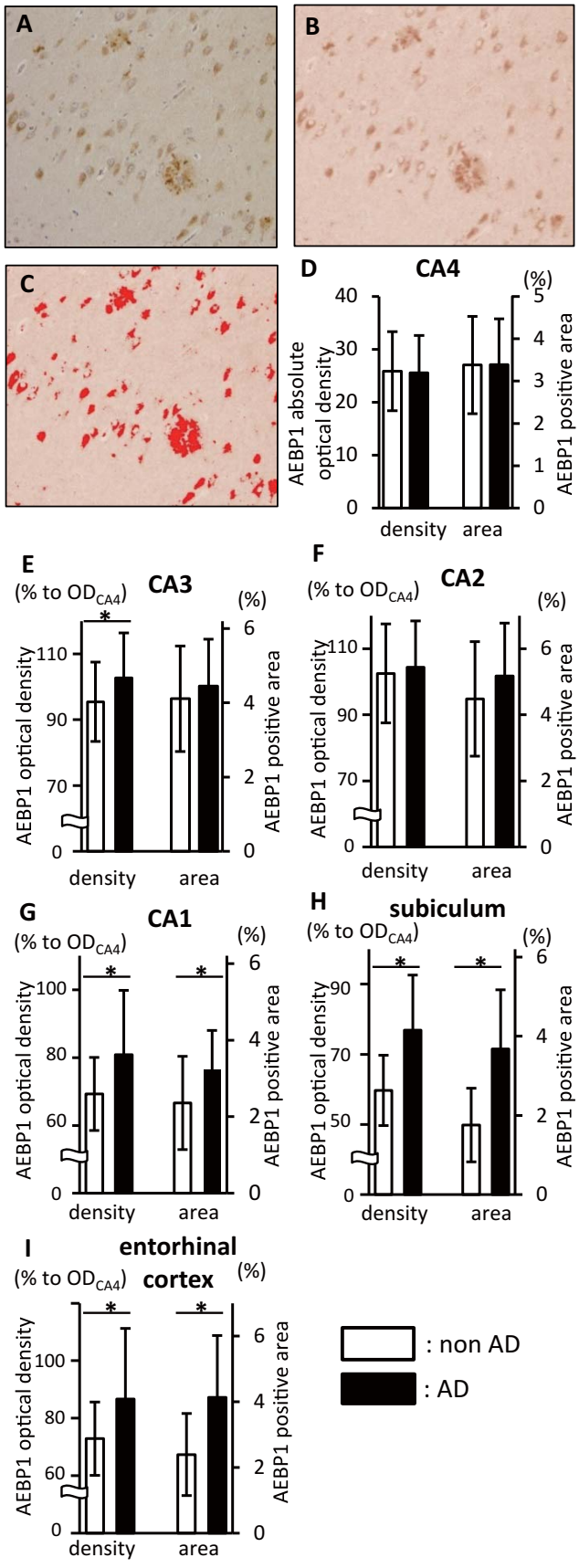

Figure 5. Semi-quantification of AEBP1-immunoreactivities in hippocampi and parahippocampal cortices. **(A)** A representative RGB image of AEBP1-immunohistochemisry from a high power view. **(B)** Extraction of DAB products using ImageJ plugin (25). **(C)** The regions of interests (ROI) for densitometry and area measurement are colored in red. **(D)** The absolute optical densities and AEBP1-immunopositive areas of AEBP1-immunohistochemistry in area CA4. There is no significant difference between non-AD cases (white columns) and AD cases (black columns). **(E–I)** The optical densities of AEBP1-immunohistochemistry (density relative to OD$_{CA4}$) and the AEBP1-positive areas in areas CA3 (**E**), CA2 (**F**) and CA1 (**G**), the subiculum (**H**), and the entorhinal cortex (**I**) of non-AD cases (white columns) and AD cases (black columns). Values are mean ± SD (*$P < 0.05$ in Welch's *t*-test). (**A-C**) Bars = 100 μm.

AEBP1 protein was deposited in senile plaques in area CA1, the subiculum and the entorhinal cortex. This was reflected in the results of immunohistochemical densitometry showing that the AEBP1-positive area increased in these regions as AD pathology progressed. In senile plaques, AEBP1 protein was distributed in club-like structures around amyloid cores, and the distribution of AEBP1 was different to that of amyloid β protein. These AEBP1-immunopositive structures were mainly located at the peripheral zone of senile plaques and were larger than microglial soma in size. Double immunofluorescence revealed that AEBP1 protein in senile plaques partially co-localized with 4-repeat tau protein, rather than glial markers. These expression patterns suggest that AEBP1 may accumulate in degenerative neurites in response to an increased concentration of tau protein. In comparison, AEBP1 protein was depleted in highly degenerated neuronal processes in senile plaques that were filled with tau tangles. Likewise, NFTs in pyramidal neurons were immunonegative for AEBP1, and AEBP1 protein appeared to be depleted in the somata of neurons with NFTs. Meanwhile, neurons with pretangles showed increased expression of AEBP1. We suggest that the increased expression of AEBP1 in senile plaques and pretangle-bearing neurons contributes to the overall increase of AEBP1protein expression in AD hippocampi. These findings also suggest that the expression of AEBP1 in hippocampal neurons may be elevated in response to pretangles, but downregulated at the advanced stage of NFT formation. Thus, it is likely that AEBP1 does not directly participate in the aggregation of tau protein. This hypothesis is also reflected in the observation that the correlation of Braak and Braak NFT stage with AEBP1 mean OD was weaker than that of the AEBP1 positive area in area CA1, the subiculum and the entorhinal cortex. Based on the amyloid cascade hypothesis, these results imply that AEBP1 in neurons and glial cells acts in response to amyloid β and tau pathology in earlier stages, but not in the later stages when tau aggregation occurs.

Immunoblotting did not reveal any difference between AD and non-AD hippocampi in the expression level of the AEBP1 protein. This was not fully consistent with the results from the mRNA expression level and IHC densitometry, each of which showed increases in AEBP1 expression in AD hippocampi. In addition, although RT-PCR has revealed that the main transcript of *AEBP1* in human hippocampi is mRNA1, coding full-length protein, immunoblotting for AEBP1 reveals bands at lower molecular weights, in addition to the bands corresponding to the full-length protein. These discrepancies might be partly attributed to the post-translational

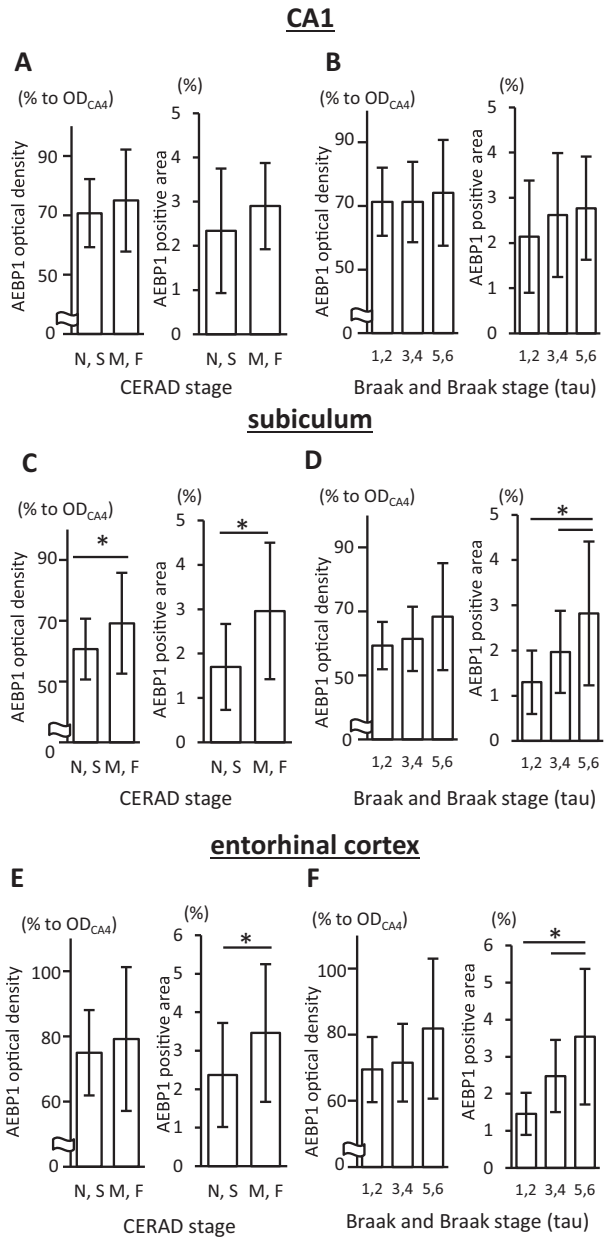

Figure 6. Increased AEBP1 immunoreactivities in subfields of the hippocampi and parahippocampal cortices (**A, B**: CA1; **C, D**: subiculum; **E, F**: entorhinal cortex) along with the severities of AD pathology. The relative optical densities of AEBP1 immunostaining in each region are shown as ratios to the densities in area CA4. The AEBP1-positive areas are shown as percentages of the total area. CERAD, The Consortium to Establish a Registry for Alzheimer's Disease; N, S, senile plaque density is "none" or "sparse"; M, F, Senile plaque density is "moderate" or "frequent." Values are mean ± SD [$*P < 0.05$ in Welch's *t*-test (A, C, E) or Tukey–Kramer HSD *post hoc* test after one-way ANOVA (B, D, F)].

processing and stability of the AEBP1 protein, as well as differences in the tissue distribution of mRNA and protein in the hippocampus. For example, in regulating NF-κB, AEBP1 is degraded, together with IκBα, by the ubiquitin-proteasome pathway (17).

The function of the AEBP1 protein in normal and AD hippocampi is still not well understood. Previous reports have shown that the full-length AEBP1 protein is mainly secreted to the extracellular matrix, and plays a role in extracellular matrix remodeling in both mouse and human (4, 5, 14, 28). In contrast, the short isoform of the mouse Aebp1 protein resides in the cytoplasm and nuclei. It modulates intracellular signaling, such as through the NF-κB pathway via degradation of IκBα (17) and the phosphatidylinositol pathway via degradation of PTEN (24), and also regulates the gene expression of *PPARG* and *NR1H2* as a transcriptional repressor (16). The short isoform of AEBP1 in humans has not been extensively studied. However, the amino acid sequence of the short isoform predicted from mRNA2 consists of the 545–1158 amino acids of the full-length protein but largely lacks the IκBα-binding site (amino acids 390–555 of the full-length protein) and one MAPK interaction site (amino acids 421–624 amino acids of the full-length protein), which are fully contained only in full-length AEBP1 (29). Thus, the short isoform of human AEBP1 might not modulate the NF-κB pathway unlike that of mouse Aebp1, and the full-length protein of human AEBP1 might be used for regulating intracellular signaling in human brain. The cytoplasmic distribution of the AEBP1 protein suggests that it modulates intracellular, extranuclear components of signaling pathways rather than acting as a transcriptional repressor in neurons and microglia. The nuclear translocation of NF-κB in neurons expressing high levels of AEBP1 is in line with this hypothesis. Previous reports have shown that the amyloid β protein stimulates neuronal and microglial Toll-like receptor 4 (TLR4), resulting in neuronal apoptosis (27, 30). There is also evidence that the TLR4-mediated PTEN/PI3K/Akt/NF-κB pathway is involved in neuroinflammatory processes in hippocampal neurons (34). Immunoblotting also revealed that there are ∼80-kDa proteins labeled by two anti-AEBP1 antibodies (recognizing amino acids 341–372 and 912–1014), suggesting fragments of full-length AEBP1 containing the IκBα-binding site (amino acids 390–555), MAPK interaction site (amino acids 421–624) and probably the PTEN-interaction site (amino acids 555–985). Together these data suggest that the AEBP1 protein might promote neuroinflammation via NF-κB and PTEN in human hippocampal neurons, and contribute to neurodegeneration. Furthermore, the neurotoxic effects of amyloid β protein- and the tau protein-mediated NF-κB pathway via reactive oxygen species (10, 31) and inflammasome (8) have been reported. Therefore, AEBP1 could also enhance these neuroinflammatory processes via IκBα degradation. Conversely, constitutive expression of the AEBP1 protein in normal human hippocampi suggests that AEBP1 also has roles in normal neuronal function and neuroprotection against pathological changes. NF-κB signaling, for example, is necessary for the regeneration of axons (6) and the maintenance of late-phase long-term potentiation and long-term memory (22).

In conclusion, the AEBP1 protein is expressed in the pyramidal neurons of human central nervous system and increased in neurons and glial cells of hippocampi and parahippocampal cortices, correlating with the progression of AD. AEBP1 could modulate neuronal and glial intracellular signaling, such as the NF-κB and PTEN pathways. AEBP1 protein accumulation in senile plaques and neurons with pretangles implies roles of AEBP1 in the progression of AD. Conversely, constitutive expression of AEBP1 in neurons suggests that AEBP1 may also have a role for normal neuronal function. Further functional

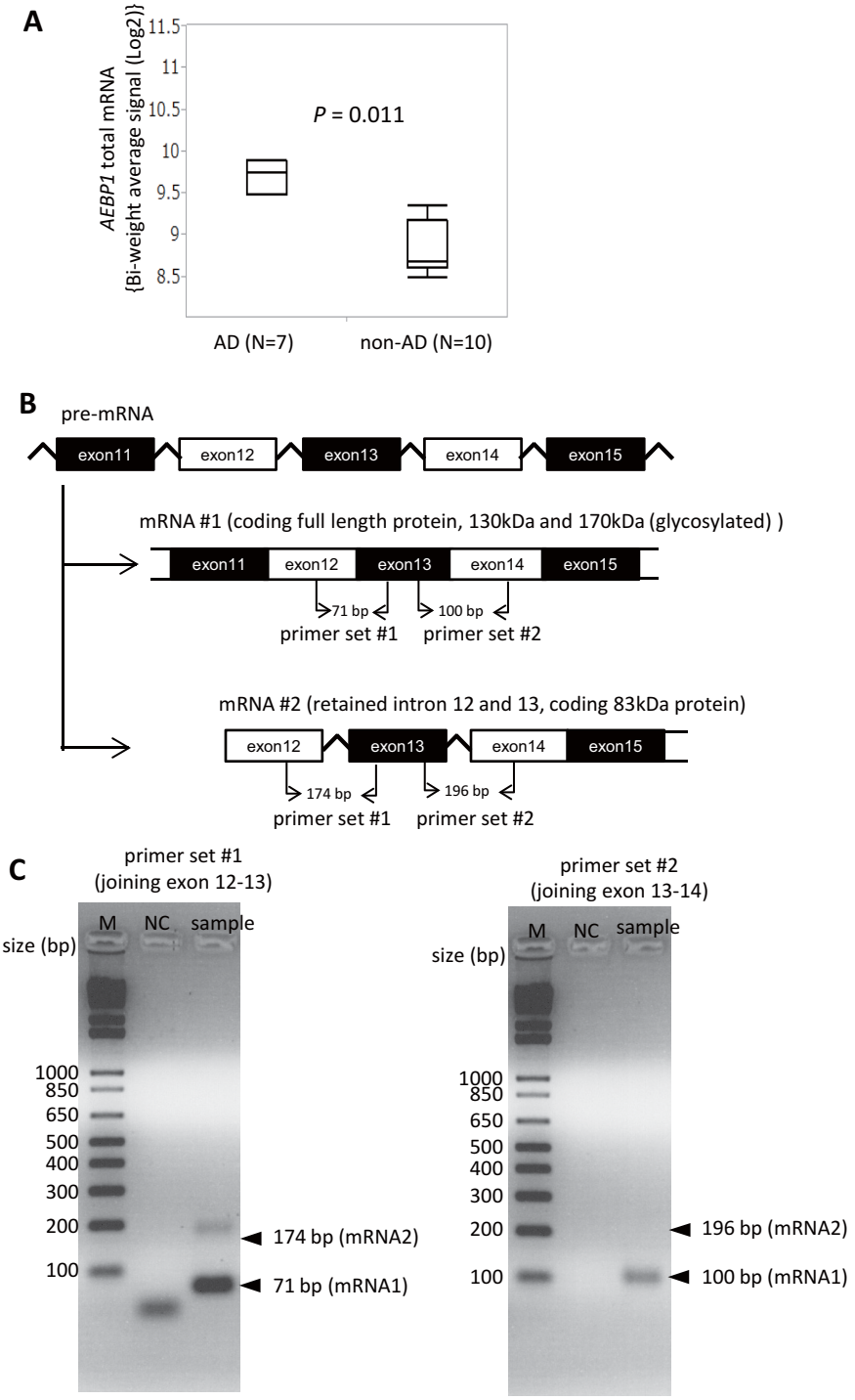

Figure 7. *AEBP1* mRNA analysis in human hippocampi. **(A)** Comparison of the expression levels of *AEBP1* mRNA between AD and non-AD cases from our previous study (9). The total amount of *AEBP1* mRNA is increased in AD cases compared with non-AD subjects. **(B)** The scheme of *AEBP1* mRNA alternative splicing and the differentiation by RT-PCR between mRNA1 and mRNA2. Human Genome Assembly build GRCh38 shows that *AEBP1* mRNA1 coding full-length protein contains 21 exons, and that exon 1 of *AEBP1* mRNA2 consists of exons 12–14 and retained introns 12 and 13. We designed primer sets flanking the junction of exons 12 and 13 (primer set #1) and exons 13 and 14 (primer set #2), so that mRNA1 and mRNA2 could be differentiated by the molecular sizes of the PCR products. **(C)** The RT-PCR products from an AD case using primer sets #1 and #2. Primer dimers are observed in the product amplified by primer set #1. The PCR products corresponding to mRNA1 are amplified by both primer sets. In contrast, the bands corresponding to mRNA2 are amplified only by primer set #1. bp: base pairs, M: 1Kb Plus DNA Ladder (Thermo Fisher Scientific, Waltham, MA, USA), NC: negative control without the template cDNA.

studies are needed to uncover the physiological and molecular biological functions of AEBP1 in human hippocampal neurons and to define the pathological role in AD.

Acknowledgments

This research was funded by the Japan Society for the Promotion of Science Grants-in-Aid for Scientific Research (KAKENHI) Grant Number 26290017 and by the Japan Agency for Medical Research and Development, AMED Grant Number 15dk0207003h0003. The authors thank Dr. Naoki Fujii (Department of Neurology, Neuro-Muscular center, National Omuta Hospital) for providing the human tissue samples of the non-demented patient, and Ms. Sachiko Koyama (Department of Neuropathology, Kyushu University) for her excellent technical assistance.

REFERENCES

1. Bogachev O, Majdalawieh A, Pan X, Zhang L, Ro HS (2011) Adipocyte enhancer-binding protein 1 (AEBP1) (a novel macrophage proinflammatory mediator) overexpression promotes and ablation attenuates atherosclerosis in ApoE (-/-) and LDLR (-/-) mice. *Mol Med* **17**:1056–1064.
2. Braak H, Braak E (1991) Neuropathological stageing of Alzheimer-related changes. *Acta Neuropathol* **82**:239–259.
3. Danzer E, Layne MD, Auber F, Shegu S, Kreiger P, Radu A *et al* (2010) Gastroschisis in mice lacking aortic carboxypeptidase-like protein is associated with a defect in neuromuscular development of the eviscerated intestine. *Pediatr Res* **68**:23–28.
4. Didangelos A, Yin X, Mandal K, Saje A, Smith A, Xu Q, Jahangiri M, Mayr M (2011) Extracellular matrix composition and remodeling in human abdominal aortic aneurysms: a proteomics approach. *Mol Cell Proteomics* **10**:M111.008128.
5. Gagnon A, Landry A, Proulx J, Layne MD, Sorisky A (2005) Aortic carboxypeptidase-like protein is regulated by transforming growth factor beta in 3T3-L1 preadipocytes. *Exp Cell Res* **308**:265–272.
6. Haenold R, Weih F, Herrmann KH, Schmidt KF, Krempler K, Engelmann C *et al* (2014) NF-kappaB controls axonal regeneration and degeneration through cell-specific balance of RelA and p50 in the adult CNS. *J Cell Sci* **127**:3052–3065.
7. He GP, Muise A, Li AW, Ro HS (1995) A eukaryotic transcriptional repressor with carboxypeptidase activity. *Nature* **378**:92–96.
8. Heneka MT, Kummer MP, Stutz A, Delekate A, Schwartz S, Vieira-Saecker A *et al* (2013) NLRP3 is activated in Alzheimer's disease and contributes to pathology in APP/PS1 mice. *Nature* **493**:674–678.
9. Hokama M, Oka S, Leon J, Ninomiya T, Honda H, Sasaki K *et al* (2014) Altered expression of diabetes-related genes in Alzheimer's disease brains: the Hisayama study. *Cereb Cortex* **24**:2476–2488.
10. Kaltschmidt B, Uherek M, Volk B, Baeuerle PA, Kaltschmidt C (1997) Transcription factor NF-kappaB is activated in primary neurons by amyloid beta peptides and in neurons surrounding early plaques from patients with Alzheimer disease. *Proc Natl Acad Sci USA* **94**:2642–2647.
11. Kim SW, Muise AM, Lyons PJ, Ro HS (2001) Regulation of adipogenesis by a transcriptional repressor that modulates MAPK activation. *J Biol Chem* **276**:10199–10206.
12. Ladha J, Sinha S, Bhat V, Donakonda S, Rao SM (2012) Identification of genomic targets of transcription factor AEBP1 and its role in survival of glioma cells. *Mol Cancer Res* **10**:1039–1051.
13. Layne MD, Endege WO, Jain MK, Yet SF, Hsieh CM, Chin MT *et al* (1998) Aortic carboxypeptidase-like protein, a novel protein with discoidin and carboxypeptidase-like domains, is up-regulated during vascular smooth muscle cell differentiation. *J Biol Chem* **273**:15654–15660.
14. Layne MD, Yet SF, Maemura K, Hsieh CM, Bernfield M, Perrella MA, Lee ME (2001) Impaired abdominal wall development and deficient wound healing in mice lacking aortic carboxypeptidase-like protein. *Mol Cell Biol* **21**:5256–5261.
15. Majdalawieh A, Ro HS (2009) LPS-induced suppression of macrophage cholesterol efflux is mediated by adipocyte enhancer-binding protein 1. *Int J Biochem Cell Biol* **41**:1518–1525.
16. Majdalawieh A, Zhang L, Fuki IV, Rader DJ, Ro HS (2006) Adipocyte enhancer-binding protein 1 is a potential novel atherogenic factor involved in macrophage cholesterol homeostasis and inflammation. *Proc Natl Acad Sci USA* **103**:2346–2351.
17. Majdalawieh A, Zhang L, Ro HS (2007) Adipocyte enhancer-binding protein-1 promotes macrophage inflammatory responsiveness by up-regulating NF-kappaB via IkappaBalpha negative regulation. *Mol Biol Cell* **18**:930–942.
18. Matsuzaki T, Sasaki K, Tanizaki Y, Hata J, Fujimi K, Matsui Y *et al* (2010) Insulin resistance is associated with the pathology of Alzheimer disease: the Hisayama study. *Neurology* **75**:764–770.
19. Matsuzaki T, Sasaki K, Hata J, Hirakawa Y, Fujimi K, Ninomiya T *et al* (2011) Association of Alzheimer disease pathology with abnormal lipid metabolism: the Hisayama Study. *Neurology* **77**:1068–1075.
20. Mirra SS, Heyman A, McKeel D, Sumi SM, Crain BJ, Brownlee LM *et al* (1991) The consortium to establish a registry for Alzheimer's disease (CERAD). Part II. Standardization of the neuropathologic assessment of Alzheimer's disease. *Neurology* **41**:479–486.
21. Ohno I, Hashimoto J, Shimizu K, Takaoka K, Ochi T, Matsubara K, Okubo K (1996) A cDNA cloning of human AEBP1 from primary cultured osteoblasts and its expression in a differentiating osteoblastic cell line. *Biochem Biophys Res Commun* **228**:411–414.
22. Oikawa K, Odero GL, Platt E, Neuendorff M, Hatherell A, Bernstein MJ, Albensi BC (2012) NF-kappaB p50 subunit knockout impairs late LTP and alters long term memory in the mouse hippocampus. *BMC Neurosci* **13**:45.
23. Ro HS, Kim SW, Wu D, Webber C, Nicholson TE (2001) Gene structure and expression of the mouse adipocyte enhancer-binding protein. *Gene* **280**:123–133.
24. Ro HS, Zhang L, Majdalawieh A, Kim SW, Wu X, Lyons PJ *et al* (2007) Adipocyte enhancer-binding protein 1 modulates adiposity and energy homeostasis. *Obesity (Silver Spring)* **15**:288–302.
25. Ruifrok AC, Johnston DA (2001) Quantification of histochemical staining by color deconvolution. *Anal Quant Cytol Histol* **23**:291–299.
26. Schissel SL, Dunsmore SE, Liu X, Shine RW, Perrella MA, Layne MD (2009) Aortic carboxypeptidase-like protein is expressed in fibrotic human lung and its absence protects against bleomycin-induced lung fibrosis. *Am J Pathol* **174**:818–828.
27. Tang SC, Lathia JD, Selvaraj PK, Jo DG, Mughal MR, Cheng A *et al* (2008) Toll-like receptor-4 mediates neuronal apoptosis induced by amyloid β-peptide and the membrane lipid peroxidation product 4-hydroxynonenal. *Exp Neurol* **213**:114–121.
28. Tumelty KE, Smith BD, Nugent MA, Layne MD (2014) Aortic carboxypeptidase-like protein (ACLP) enhances lung myofibroblast differentiation through transforming growth factor beta receptor-dependent and -independent pathways. *J Biol Chem* **289**:2526–2536.
29. UniProt Consortium (2015) UniProt: a hub for protein information. *Nucleic Acids Res* **43**:D204–D212.
30. Walter S, Letiembre M, Liu Y, Heine H, Penke B, Hao W *et al* (2007) Role of the toll-like receptor 4 in neuroinflammation in Alzheimer's disease. *Cell Physiol Biochem* **20**:947–956.
31. Yan SD, Yan SF, Chen X, Fu J, Chen M, Kuppusamy P *et al* (1995) Non-enzymatically glycated tau in Alzheimer's disease

induces neuronal oxidant stress resulting in cytokine gene expression and release of amyloid beta-peptide. *Nat Med* **1**: 693–699.
32. Yates A, Akanni W, Amode MR, Barrell D, Billis K, Carvalho-Silva D, Cummins C, Clapham P, Fitzgerald S, Gil L, Giron CG, Gordon L, Hourlier T, Hunt SE, Janacek SH, Johnson N, Juettemann T, Keenan S, Lavidas I, Martin FJ, Maurel T, McLaren W, Murphy DN, Nag R, Nuhn M, Parker A, Patricio M, Pignatelli M, Rahtz M, Riat HS, Sheppard D, Taylor K, Thormann A, Vullo A, Wilder SP, Zadissa A, Birney E, Harrow J, Muffato M, Perry E, Ruffier M, Spudich G, Trevanion SJ, Cunningham F, Aken BL, Zerbino DR, Flicek P (2016) Ensembl 2016. *Nucleic Acids Res* **44**:D710–D716.
33. Zhang L, Reidy SP, Nicholson TE, Lee HJ, Majdalawieh A, Webber C *et al* (2005) The role of AEBP1 in sex-specific diet-induced obesity. *Mol Med* **11**:39–47.
34. Zhao M, Zhou A, Xu L, Zhang X (2014) The role of TLR4-mediated PTEN/PI3K/AKT/NF-kappaB signaling pathway in neuroinflammation in hippocampal neurons. *Neuroscience* **269**: 93–101.

SUPPORTING INFORMATION

Additional Supporting Information may be found in the online version of this article at the publisher's web-site:

Figure S1. Examples of semi-quantification for AEBP1-immunopositivity. **(−)**: No AEBP1-immunopositive structures. **(+)**: Over half of the cells weakly immunopositive for AEBP1. **(++)**: Many of the cells immunopositive for AEBP1 with variable staining intensities. **(+++)**: Almost all cells are strongly immunopositive for AEBP1. Bars = 20 μm and 100 μm.

Figure S2. Immunohistochemistry without primary antibody in human hippocampi and parahippocampal cortices of an AD case, as a negative control. **(A)** Low-power images of CA2–CA4 subfields. **(B–G)** Immunostaining in the CA4 region (**B**), CA3 (**C**), CA2 (**D**), CA1 (**E**), subiculum (**F**) and dentate gyrus (**G**). (**H**) Immunostaining at senile plaques in the subiculum. There is faint, non-specific staining of lipofuscin in pyramidal neurons. However, the strongly stained structures shown in Figures 1–3 and S3 are not observed. **A**: bars = 500 μm. **B–H**: bars = 20 μm.

Figure S3. Distribution of AEBP1 protein expression in astrocytes and microglia. **(A)** Bright-field view of astrocytes immunolabeled for AEBP1. **(B–M)** Immunofluorescence for AEBP1 (green) and the astrocyte markers GFAP and S-100 protein (red) in single cells **(B–G)** and a senile plaque **(H–M)**. **(N)** Bright-field view of microglia immunolabeled for AEBP1. **(O–Z)** Immunofluorescence for AEBP1 (green) and the microglia markers Iba-1 and LCA (red) in single cells **(O–T)** and a senile plaque **(U–Z)**. Immunohistochemistry shows that some astrocytes and microglia express AEBP1 in the perinuclear cytosol (arrows), whereas the AEBP1-immunopositive structures in senile plaques (arrowhead) are not located in astrocytes or microglia. Bars = 20 μm.

Figure S4. Western blotting for AEBP1. **(A)** AEBP1-immunoblotting with an antibody recognizing the C-terminus of AEBP1 (ab54820) on human tissue lysates from a non-demented control subject. Lane 1, aorta; lane 2, adrenal gland; lane 3, hippocampus; lane 4, frontal cortex. Immunoblotting of human aorta (lane 1) shows several bands, which may correspond to the protein translated from the mRNA2 splice variant (83 kDa), the full-length form (130 kD) and its glycosylated form (170 kD). Each 83-kDa, 130-kDa and 170-kDa band is indicated by arrowheads. Immunoblotting of adrenal gland tissue (lane 2), shows a major band at 83 kDa, whereas the bands corresponding to the full-length form are not evident. Immunoblotting of the hippocampus (lane 3) and frontal cortex (lane 4) show major bands at 83 kDa and a band at 170 kDa. The other bands are believed to be degradation products and non-specific bands, such as serum immunoglobulin. **(B)** AEBP1-immunoblotting of hippocampal lysates diluted in radioimmunoprecipitation assay buffer from four AD and four non-AD subjects from our previous study (9). Immunoblotting with an antibody recognizing the C-terminus of AEBP1 (ab54820) shows that there are also weak bands around 83 kDa and 170 kDa. The entire protein blot of the samples indicated by asterisks is shown below. These bands around 83 kDa and 170 kDa are also seen when immunoblotting with an antibody recognizing the N-terminus of AEBP1 (LS-C156122). M: MagicMark™ XP Western Protein Standard (ThermoFisher Scientific, Waltham, MA, USA)